

Nano-mechanical oscillations in a single-C₆₀ transistor

Hongkun Park*[‡]§, Jiwoong Park[†], Andrew K. L. Lim*, Erik H. Anderson[‡], A. Paul Alivisatos*[‡] & Paul L. McEuen[†]‡

* Department of Chemistry and [†] Department of Physics, University of California at Berkeley, and [‡] Materials Sciences Division, Lawrence Berkeley National Laboratory, Berkeley, CA 94720, USA

Over the last decade, electron transport through quantum dots has attracted considerable attention from the scientific and engineering community. The electronic motion through these structures is strongly modified by single-electron charging and energy level quantization^{1,2}. Recently, much effort has been directed toward extending these studies to chemical nanostructures, such as molecules³⁻⁸, nanocrystals⁹⁻¹³, and nanotubes¹⁴⁻¹⁷. Here we report for the first time the fabrication of single-molecule transistors based on individual C₆₀ molecules. Transport measurements of single-C₆₀ transistors provide evidence for coupling between the center-of-mass motion of C₆₀ and single-electron hopping¹⁸, a novel conduction mechanism that has not been observed in previous quantum-dot studies. This coupling manifests itself as quantized nano-mechanical oscillations of C₆₀ against the gold surface. The frequency of this oscillation is determined to be around 1.2 THz, in excellent agreement with a simple theoretical estimate based on van der Waals and electrostatic interactions between C₆₀ and gold electrodes.

Single-C₆₀ transistors were prepared by depositing a dilute toluene solution of C₆₀ onto a pair of connected gold electrodes fabricated using e-beam lithography. A break-junction technique¹¹ was then used to create a ~1 nm gap between these electrodes by the process of electromigration. In a significant fraction of these devices, the conductance of the junction after initial breaking is substantially enhanced compared to devices with no C₆₀ deposited, indicating that C₆₀ molecules reside in the junction. The entire structure was defined on a SiO₂ insulating layer on top of a degenerately doped silicon wafer which serves as a gate electrode that modulates the electrostatic potential of C₆₀. A schematic diagram of an idealized single-C₆₀ transistor is shown in the lower inset of Fig. 1.

Figure 1 presents representative current-voltage (*I-V*) curves obtained from a single-C₆₀ transistor at different gate voltages (*V_g*). The device exhibited strongly suppressed conductance near zero bias voltage followed by step-like current jumps at higher voltages. The voltage width of the zero-conductance region (conductance gap) could be changed in a reversible manner by changing *V_g*. In ten devices prepared from separate fabrication runs, the conductance gap could be reduced to zero by adjusting *V_g*, although the gate voltage at which the conductance gap closed (*V_c*) varied from device to device.

Figures 2 and 3 show two-dimensional plots of differential conductance ($\partial I/\partial V$) as a function of both *V* and *V_g* for four different devices. Peaks in $\partial I/\partial V$, which correspond to the step-like features in Fig. 1, show up as lines in these plots. As seen clearly in Figs. 2 and 3, the size of the conductance gap and the $\partial I/\partial V$ peak positions evolve smoothly as *V_g* is varied. As the gate voltage was varied farther away from *V_c* in both positive and negative directions, the conductance gap continued to widen and exceeded $|V| \geq 150$ mV in some devices. Many

$\partial I/\partial V$ peaks outside the conductance gap are also observed.

The *V_g*-dependent features described above were not observed in devices when C₆₀ was not deposited on the electrodes. In addition, many different devices exhibited similar conductance characteristics, as shown in Fig. 2. Furthermore, the observed behavior is consistent with a single nanometer-sized object bridging two electrodes, as explained in detail below¹. Although C₆₀ could not be imaged directly in these devices due to its small size (~7 Å in diameter), these experimental observations indicate that individual C₆₀ molecules are responsible for the conductance features observed in the experiment.

The global patterns observed in Figs. 1 - 3 can be understood using ideas borrowed from the Coulomb blockade model developed for the analysis of quantum-dot transport¹. The conductance gap observed in the data is a consequence of the finite energy required to add (remove) an electron to (from) C₆₀. This energy cost arises from the combined effect of single-electron charging of C₆₀ and the quantized excitation spectrum of the C₆₀-transistor system. The maximum observed gap in the experiment indicates that the charging energy of the C₆₀ molecule in this geometry can exceed 150 meV.

The conductance gap changes reversibly as a function of *V_g* because more positive gate voltage stabilizes an additional electron on C₆₀. The conductance gap disappears at *V_g* = *V_c* where the electrochemical potential becomes identical for two different C₆₀ charge states. When the gate voltage traverses *V_c* in the positive direction, the equilibrium number of charges on C₆₀ changes by one electron from C₆₀^{*n*-} to C₆₀^{*n*+1}, where *n* designates the number of charges on C₆₀. It is determined by both *V_g* and the local electrochemical environment, that is the work function of the metal electrode and the local charge

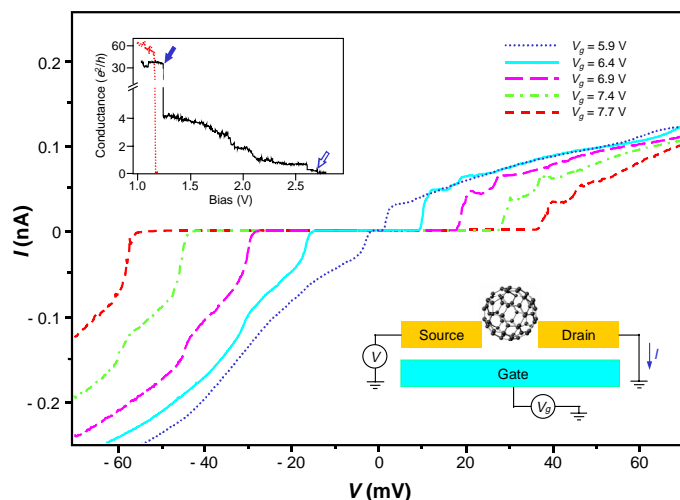


Figure 1 Current-voltage (*I-V*) curves obtained from a single-C₆₀ transistor at *T* = 1.5 K. Five *I-V* curves taken at different gate voltages (*V_g*) are shown. Single-C₆₀ transistors were prepared first by depositing a dilute toluene solution of C₆₀ onto a pair of connected gold electrodes. A ~1 nm gap was then created using electromigration-induced breaking of the electrodes. A large bias was applied between the electrodes while the conductance between them was monitored (black solid curve, upper inset). After the initial rapid decrease (solid arrow), the conductance stayed above the conductance quantum ($e^2/h = 38.7 \mu\text{S}$) until ~ 2.0 V. This large residual conductance was observed in most single-C₆₀ transistors, but was not observed when no C₆₀ solution was deposited (red dotted curve). The bias voltage was increased until the conductance fell significantly below e^2/h (open arrow) to ensure that the current through the junction is in the tunneling regime. The low bias measurements shown in the main panel were taken after the breaking procedure. The lower inset depicts the schematic diagram of an idealized single-C₆₀ transistor formed by this method.

§ Present Address: Department of Chemistry and Chemical Biology, Harvard University, Cambridge, MA 02138, USA

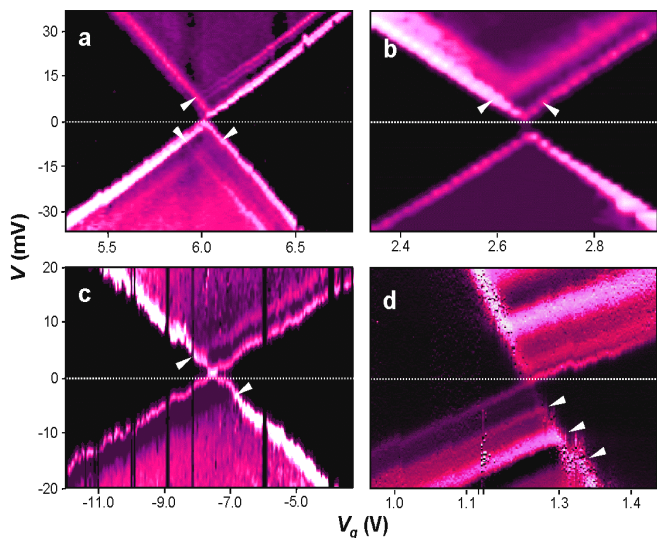


Figure 2 Two-dimensional differential conductance ($\partial I/\partial V$) plots as a function of the bias voltage (V) and the gate voltage (V_g) obtained from four different devices prepared from separate fabrication runs. The dark triangular regions correspond to the conductance gap, and the bright lines represent peaks in the differential conductance. The differential conductance values are represented by the color scale, which changes from black (0 nS) through pink to white (white representing 30 nS in **a**, **b**, **c** and 5 nS in **d**). The white arrows mark the point where $\partial I/\partial V$ lines intercept the conductance gap. During the acquisition of data in **d**, one “switch” where the entire $\partial I/\partial V$ characteristics shift along the V_g axis occurred at $V_g = 1.15$ V. The right portion of the plot **d** is shifted along the V_g axis to preserve the continuity of the lines.

distribution around C_{60} . While the value of n cannot be determined solely from our experimental data, previous electrochemical and photoelectron spectroscopic studies of C_{60} on gold suggest that n is most likely zero or one¹⁹.

The position of each $\partial I/\partial V$ peak outside the conductance gap in Figs. 2 and 3 provides detailed information on the quantized excitations of the single- C_{60} transistor system¹. These $\partial I/\partial V$ peaks appear when a new quantized excitation becomes energetically accessible, providing an electron-tunneling pathway between C_{60} and the gold electrodes. Specifically, each $\partial I/\partial V$ peak on the $V_g < V_c$ side signifies an opening of a new tunneling pathway where an electron hops onto C_{60}^{n-} to generate $C_{60}^{(n+)-}$ in its ground or excited states; these peaks therefore probe the excitation energies of the $C_{60}^{(n+)-}$ ion. Each $\partial I/\partial V$ peak that appears at $V_g > V_c$ occurs when an electron hops off $C_{60}^{(n+)-}$ to generate C_{60}^{n-} ; these peaks thus probe the ground and excited states of C_{60}^{n-} . The energy of these quantized excitations can be determined from the bias voltage at which they intercept the conductance gap¹, as shown by the white arrows in Fig. 2.

A remarkable common feature of the different devices is that a quantized excitation is universally observed with an energy of ~ 5 meV. Moreover, this excitation is observed on both sides of V_c in most devices, indicating that it is an excitation of both charge states of C_{60} . The exact value of this energy quantum varied from device to device and ranged from 3 to 7 meV. In some devices, multiple $\partial I/\partial V$ features with almost identical spacing appear, as seen in Fig. 2d.

The observed 5-meV excitation could arise from many possible degrees of freedom of the single- C_{60} transistor system. One possibility, which has been commonly invoked in other nanometer-scale systems, is the excited electronic states of the system. However, this possibility can be ruled out here based on the observation that the 5-meV excitation is

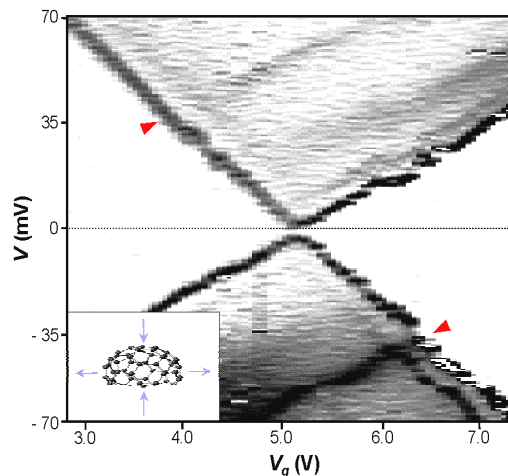


Figure 3 A differential conductance plot showing a larger bias-voltage range than those in Fig. 2. Here two $\partial I/\partial V$ lines that intercept the conductance gap at $V = 35$ mV are seen clearly (red arrows). The energy quantum of this excitation closely matches that of the C_{60} internal vibrational mode shown in the inset.

the same for both charge states of C_{60} and that multiple excitations with the same spacing are observed. Although the exact electronic-level structures of the C_{60}^{n-} ions are not known experimentally, theoretical calculations predict that the electronic states do not follow such behavior¹⁹.

A more natural candidate is a vibrational excitation of the C_{60} system coupled to an electron tunneling on and off C_{60} . The observation of multiple $\partial I/\partial V$ features with identical spacing would then result from the excitation of integer numbers of vibrational quanta. Moreover, these vibrational modes would be present irrespective of the charge state of the C_{60} .

The internal vibrational modes of the free C_{60} molecule have been extensively studied, both theoretically and experimentally^{19,20}. The lowest-energy mode is one with a vibrational quantum of 33 meV and corresponds to the C_{60} deformation from a sphere to a prolate ellipsoid, as shown in the inset to Fig. 3. In Figure 3, an excitation that likely corresponds to this mode can indeed be seen with an energy of ~ 35 meV. However, internal vibrational modes cannot account for the observed 5-meV features.

Another possibility is the center-of-mass oscillation of C_{60} within the confinement potential that binds it to the gold surface, as shown in Fig. 4. To our knowledge, this mode has not been directly measured experimentally. However, previous theoretical and experimental studies have shown that C_{60} is held tightly on gold by van der Waals interactions, with a C_{60} -gold binding energy of ~ 1 eV and a distance of ~ 6.2 Å between the C_{60} center and the gold surface^{19,21,22}. Assuming that the C_{60} -gold interaction potential can be expressed by the Lennard-Jones form²², the above parameters can be used to determine the shape of the potential that describes the C_{60} -gold binding. This calculation indicates that the C_{60} -gold binding near the equilibrium position can be approximated very well by a harmonic potential with an estimated force constant of $k \sim 70$ N/m, as is shown schematically in Fig. 4. This force constant and the mass M of the C_{60} molecule yield a vibrational frequency of $f = (1/2\pi)(k/M)^{1/2} \sim 1.2$ THz and a vibrational quantum of $hf \sim 5$ meV, where h is the Planck constant.

Adding an additional electron to C_{60} compresses the C_{60} -surface bond due to the interaction between the C_{60} ion and its image charge in the metal. A simple estimate indicates that an additional electron on C_{60} results in the shortening of the C_{60} -surface distance by $\delta \sim 4$ pm, but it does not significantly change the vibrational frequency. By comparison,

the root-mean squared displacement x_m of the C_{60} molecule in the m -th vibrational level is given by $x_m = (2m+1)^{1/2}x_0$, where $x_0 = (hf/k)^{1/2} \sim 3$ pm.

The C_{60} -surface vibration discussed above can account for the 5-meV conductance features in a unifying fashion. The first $\partial I/\partial V$ peak at the boundary of the conductance-gap region is observed when an electron hops on or off C_{60} with the system staying in the ground vibrational level. Additional $\partial I/\partial V$ peaks on the $V_g < V_c$ side appear when an electron hops onto C_{60}^{n-} to generate $C_{60}^{(n+)-}$ in excited vibrational states. The $\partial I/\partial V$ peaks on the $V_g > V_c$ side signify, on the other hand, an event where an electron hops off $C_{60}^{(n+)-}$, leaving C_{60}^{n-} in excited vibrational levels. Multiple $\partial I/\partial V$ peaks on the same side of V_c indicate that more than one vibrational quantum are excited.

This process is thus reminiscent of the Franck-Condon processes encountered in electron-transfer and light-absorption processes in molecules, where the vibrational excitation accompanies the electronic motion²³. Within the harmonic approximation, the vibrational matrix elements for these processes can be readily calculated, and the ratio δ/x_0 determines the number of vibrational quanta typically excited by the tunneling electron. According to the estimates discussed above, $\delta/x_0 \sim 1$ in a single- C_{60} transistor. The number of $\partial I/\partial V$ peaks visible in Fig. 2 generally confirms this expectation since only a few $\partial I/\partial V$ peaks are observed in most devices.

One device that does not follow this general trend is the one shown in Fig. 2d. As described previously, this device exhibits many $\partial I/\partial V$ peaks on both sides of V_c . In addition, the peak intensities do not show simple variations expected from the single-mode Franck-Condon picture²³. The anomalous behavior may be related to the highly asymmetric coupling of C_{60} and the two electrodes in this particular device. This asymmetry is demonstrated by the different slopes of the upward and downward $\partial I/\partial V$ lines in the $V-V_g$ plane. The variations of peak intensities may be due to the presence of other degrees of freedom in the system, such as the C_{60} motion perpendicular to the surface normal.

Unexplained features exist in other devices as well. In the data in

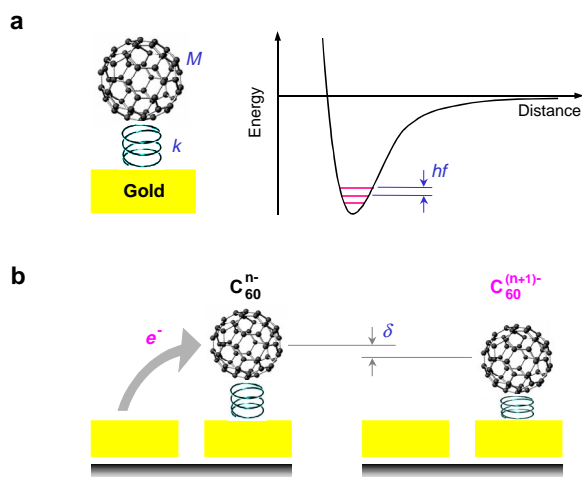


Figure 4 Schematic of the center-of-mass oscillation of C_{60} . **a**, A C_{60} molecule is bound to the gold surface by the van der Waals and electrostatic interaction. The interaction potential is schematically illustrated in the figure. The potential near the equilibrium position can be approximated well by a harmonic potential with a force constant k . This harmonic potential gives quantized energy levels with frequency $f = (1/2\pi)(k/M)^{1/2}$. Here M represents the mass of C_{60} and h is the Planck constant. **b**, When an electron jumps on to C_{60}^{n-} , the attractive interaction between the additional electron and its image charge on gold pulls the C_{60} ion closer to the gold surface by the distance δ . This electrostatic interaction results in the mechanical motion of C_{60} .

Figure 2a, a small (≤ 1 meV) energy splitting is observed for many of the lines. This splitting may arise from the C_{60} center-of-mass motion perpendicular to the surface normal discussed above. Unfortunately, the nature of the potential for this motion is not known due to the lack of detailed knowledge of the electrode geometry near C_{60} , and quantitative support of this assignment is thus lacking at present.

The coupling between the electronic and mechanical degrees of freedom is likely to be important in electron transport through nanomolecular systems^{24,25}. The transport measurements presented here demonstrate that single-electron-tunneling events can be used both to excite and probe the motion of a molecule: indeed, the single- C_{60} transistor behaves as a high-frequency nano-mechanical oscillator. Furthermore, the oscillations of the C_{60} molecule must be treated in a quantized fashion, showing that this is a true quantum-“mechanical” system.

1. Grabert, H. & Devoret, M.H. *Single Charge Tunneling* (Plenum Press, New York, 1992).
2. Sohn, L.L., Kouwenhoven, L.P. & Schön, G. *Mesoscopic Electron Transport* (Kluwer Academic Publishers, Dordrecht, 1997).
3. Bumm, L.A., *et al.* Are single molecular wires conducting? *Science* **271**, 1705 (1996).
4. Reed, M.A., Zhou, C., Muller, C.J., Burgin, T.P. & Tour, J.M. Conductance of a molecular junction. *Science* **278**, 252 (1997).
5. Datta, S., *et al.* Current-voltage characteristics of self-assembled monolayers by scanning tunneling microscopy. *Phys. Rev. Lett.* **79**, 2530 (1997).
6. Porath, D., Levi, Y., Tarabiah, M. & Millo, O. Tunneling spectroscopy of isolated C_{60} molecules in the presence of charging effects. *Phys. Rev. B* **56**, 9829 (1997).
7. Joachim, C. & Gimzewski, J.K. An electromechanical amplifier using a single molecule. *Chem. Phys. Lett.* **265**, 353 (1997).
8. Stipe, B.C., Rezaei, M.A. & Ho, W. Single-molecule vibrational spectroscopy and microscopy. *Science* **280**, 1732 (1998).
9. Klein, D.L., McEuen, P.L., Bowen Katari, J.E., Roth, R. & Alivisatos, A.P. An approach to electrical studies of single nanocrystals. *Appl. Phys. Lett.* **68**, 2574 (1996).
10. Klein, D.L., Roth, R., Lim, A.K.L., Alivisatos, A.P. & McEuen, P.L. A single-electron transistor made from a cadmium selenide nanocrystal. *Nature* **389**, 699 (1997).
11. Park, H., Lim, A.K.L., Park, J., Alivisatos, A.P. & McEuen, P.L. Fabrication of metallic electrodes with nanometer separation by electromigration. *Appl. Phys. Lett.* **75**, 301 (1999).
12. Banin, U., Cao, Y., Katz, D. & Millo, O. Identification of atomic-like electronic states in indium arsenide nanocrystal quantum dots. *Nature* **400**, 542 (1999).
13. Kim, S.-H., Medeiros-Ribeiro, G., Ohlberg, D.A.A., Williams, R.S. & Heath, J.R. Individual and collective electronic properties of Ag nanocrystals. *J. Phys. Chem. B* **103**, 10341 (1999).
14. Bockrath, M., *et al.* Single-electron transport in ropes of carbon nanotubes. *Science* **275**, 1922 (1997).
15. Tans, S.J., *et al.* Individual single-wall carbon nanotubes as quantum wires. *Nature* **386**, 474 (1997).
16. Tans, S.J., Verschueren, A.R.M. & Dekker, C. Room-temperature transistor based on a single carbon nanotube. *Nature* **393**, 49 (1998).
17. Bockrath, M., *et al.* Luttinger-liquid behavior in carbon nanotubes. *Nature* **397**, 598 (1999).
18. Gorelik, L.Y., *et al.* Shuttle mechanism for charge transfer in Coulomb blockade nanostructures. *Phys. Rev. Lett.* **80**, 4526 (1998).
19. Dresselhaus, M.S., Dresselhaus, G. & Eklund, P.C. *Science of Fullerenes and Carbon Nanotubes* (Academic Press, New York, 1996).
20. Heid, R., Pintschovius, L. & Godard, J.M. Eigenvectors of internal vibrations of C_{60} : Theory and experiment. *Phys. Rev. B* **56**, 5925 (1997).
21. Chavy, C., Joachim, C. & Altibelli, A. Interpretation of STM images: C_{60} on the gold(110) surface. *Chem. Phys. Lett.* **214**, 569 (1993).
22. Ruoff, R.S. & Hickman, A.P. van der Waals binding of Fullerenes to a graphite plane. *J. Phys. Chem.* **97**, 2494 (1993).
23. Poncharal, P., Wang, Z.L., Ugarte, D. & Heer, W.A. Electrostatic deflections and electromechanical resonances of carbon nanotubes. *Science* **283**, 1513 (1999).
24. Reulet, B., *et al.* Bolometric detection of mechanical bending waves in suspended carbon nanotubes. *Cond-mat Archive/9907486* (1999).

Acknowledgments

We thank Michael S. Fuhrer and Ned S. Wingreen for valuable discussions and advice. This work was supported by the US Department of Energy. E.A. was also partially supported by DARPA.

Correspondence and requests for materials should be addressed to P.M. (e-mail: mceuen@socrates.berkeley.edu).